Kα x-ray satellite and hypersatellite intensity distributions
of vanadium metal and oxides excited in heavy ion collisions

R. L. Watson, V. Horvat, and Y. Peng

Previous work has shown that the intensity distributions of Kα x-ray satellites arising from the decay of collision-produced excited states containing single K- plus additional L-shell vacancies are sensitive to the chemical environment for elements in the third row of the periodic table [1,2]. The origin of this chemical effect has been attributed to L vacancy transfer processes occurring between the time of collision and the time of x ray emission. In particular, fast transitions from higher levels to the L shell can change the number of L vacancies present when a K x ray is emitted. Furthermore, inter-atomic transitions from neighboring atoms can significantly contribute to the L-vacancy quenching process. For third row elements, transitions to the L shell must involve valence electrons and hence the chemical environment can be expected to have a direct influence on the rates of both intra-atomic and inter-atomic vacancy transfer.

So far, similar chemical effects have not been reported for fourth row elements. The valence shell of these elements is the N shell, which implies that inner shell x-ray transitions will be less sensitive to the chemical environment. However, chemical bonding in the fourth row transition elements involves the 3d electrons and this fact has led to extensive investigations of the dependence on oxidation state of their Kβ x-ray structure excited by electrons, photons, and protons (see for example Refs. 3 and 4). These studies have revealed significant changes in the relative intensities of the various Kβ components.

Recently we have measured the Kα x-ray spectra of vanadium metal and three of its oxides (VO, V_2O_4, and V_2O_5), excited by 15 MeV/amu Ne, Ar, Kr, Ag, and Ho ions, in order to examine the Kα x-ray satellite and hypersatellite intensity distributions for evidence of a chemical dependence. Vanadium was chosen as the target element because the energy region covered by its K x-ray spectrum could be accessed with good resolution by second order diffraction using a LiF crystal. In addition, its Kα satellites and hypersatellites are well separated from each other and from the Kβ diagram/satellite peaks. A spectrum obtained with 15 MeV/amu Kr ions incident on vanadium metal is shown in Fig. 1. The $K\alpha_{1,2}$ (or KL^0) and $K\beta_{1,3}$ diagram peaks (solid green lines) are predominately excited by secondary electrons and x-rays, while the major features of interest here, the satellite and hypersatellite distributions (dashed blue lines), are produced by heavy ion collisions in which single and double K plus additional L vacancies are created, respectively.

The spectra were corrected for absorption and detector efficiency, and fit with Voigt functions as shown in Fig. 1. The apparent average L-vacancy fractions, p_L^x, (defined in the preceding report) were calculated directly from the measured satellite and hypersatellite intensities. In the case of the satellites, it was necessary to estimate the intensity of the collision-produced component of the KL^0 peak by fitting the satellite intensities to a binomial distribution. Since the vanadium oxide targets were thick compressed pellets, care was taken to accurately account for the x-ray production and absorption cross sections in calculating the average projectile energy associated with the measured x-ray spectra.
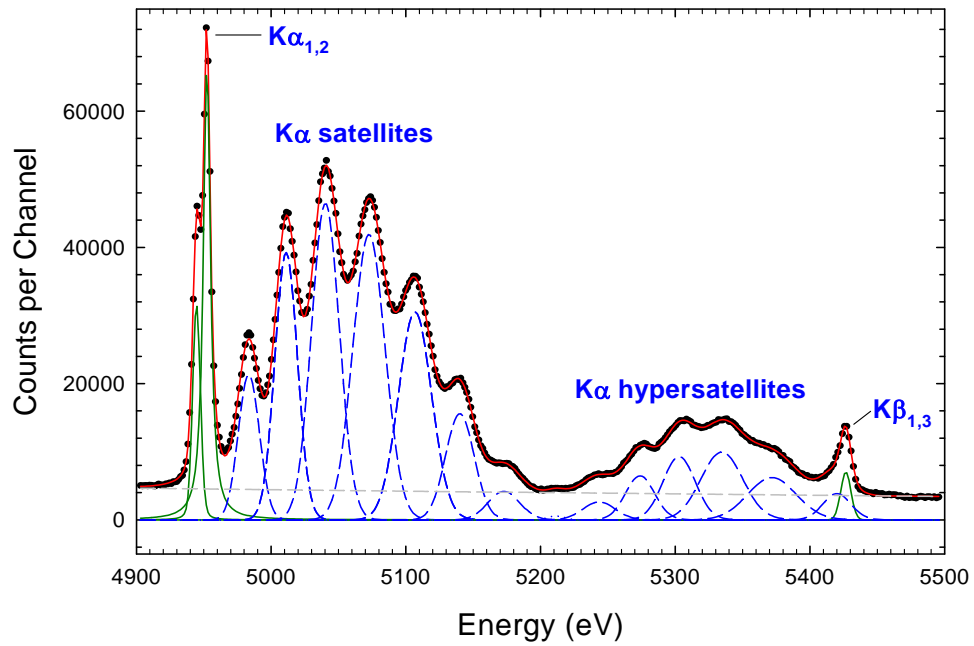
Figure 1. Spectrum of vanadium Kα x rays excited by 15 MeV/amu Kr ions incident on a vanadium metal target. The solid (red) curve through the data points shows the overall fit to the data.
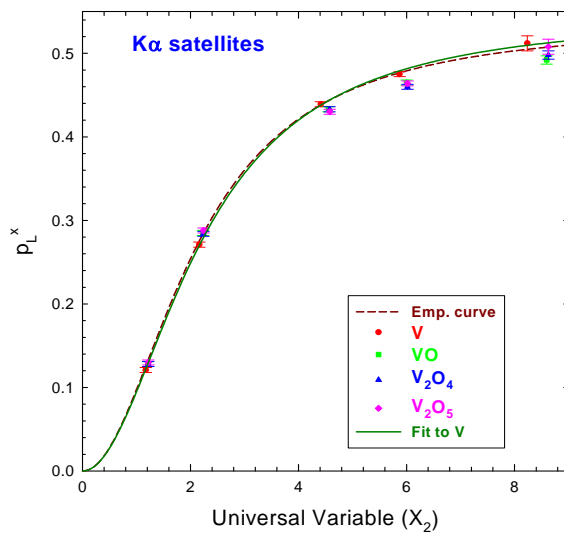

Figure 2. Comparison of the apparent average L-vacancy fractions for the satellites of vanadium metal and oxides as a function of the geometric model parameter. The solid (green) curve shows a fit to the vanadium metal points and the dashed (brown) curve shows the empirical curve determined previously [5] for a variety of metal targets.

The Kα x-ray satellite results are shown in Fig. 2 in the form of a plot of p_L^x as a function of the geometric model variable X_2 (see preceding report). Based on our previous work with metal targets [5], we expect the vanadium metal values to lie on an empirical curve shown by the dashed (brown) line. The solid (green) line was fit to the vanadium metal points and shows very good agreement with the empirical curve. The relatively low p_L^x value data points for the vanadium oxides (obtained using Ne and Ar projectiles) are displaced from the corresponding vanadium metal points due to projectile energy loss, but they fall on the same curve. This indicates that their satellite distributions are identical to those that would be obtained for vanadium metal using projectiles of the same average energy. However, the oxide p_L^x values obtained with the higher atomic number projectiles fall significantly and systematically below the curve defined by the metal data points. (It should be noted that the data points for Ho projectiles have much larger error bars than the rest due to low counting statistics caused by the limited beam intensity that was available). Although the effect is small, it may be concluded that, as the L-vacancy fraction increases, the oxides become somewhat more efficient at filling L vacancies than the metal

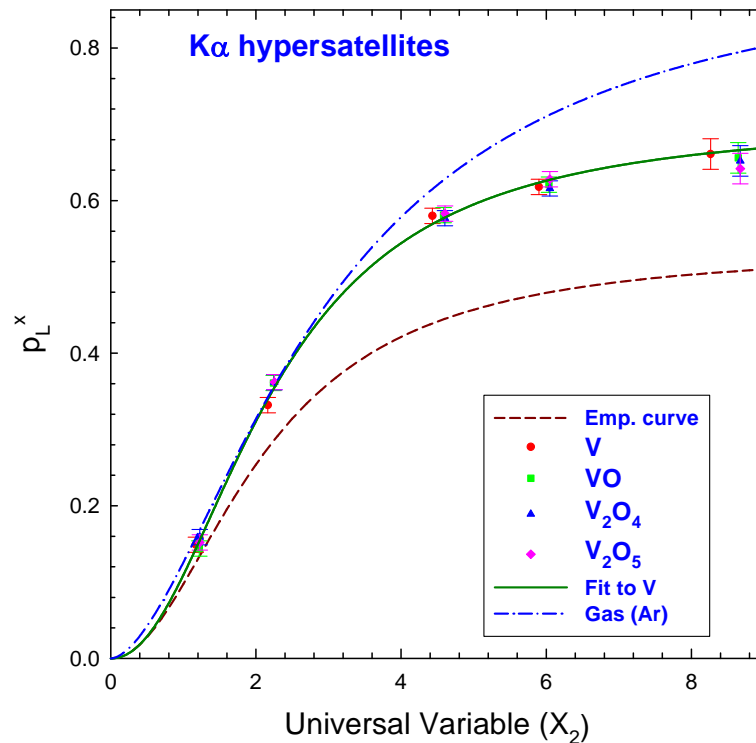The results obtained for the Kα x-ray hypersatellites are shown in Fig. 3. Unfortunately, the low

Figure 3. Comparison of the apparent average L-vacancy fractions for the hypersatellites of vanadium metal and oxides as a function of the geometric model parameter. The solid (green) curve shows a fit to the vanadium metal points, the dashed (brown) curve shows the empirical satellite curve, and the dot-dashed (blue) curve is a fit to the Ar (gas) hypersatellite data from the preceding report.

intensities of the hypersatellites and the accompanying larger error bars prevent as sensitive a test as was possible for the satellites. Considering the experimental error, it must be concluded that there is no evidence of a chemical effect for the hypersatellite intensity distributions. However, it is apparent from a comparison of the fitted hypersatellite curve (green) with the empirical satellite curve (brown) that, for solid targets, the p_L^x values of the hypersatellites are much larger than those of the satellites. Furthermore, comparison of the solid (green) curve with the dot-dashed (blue) curve in Fig. 3 (from the Ar data discussed in the preceding report) shows there is an even larger increase in the p_L^x values for the higher atomic number projectiles going from solid targets to gaseous targets, in which inter-atomic transitions cannot occur.

[1] R. L. Watson, A. K. Leeper, B. I. Sonobe, T. Chiao, and F. E. Jenson, Phys. Rev. A **15**, 914 (1977).
[2] J. A. Demarest and R. L. Watson, Phys. Rev. A **17**, 1302 (1978).
[3] S. D. Gamblin and D. S. Urch, J. Elect. Spectrosc. And Rel. Phenom. **113**, 179 (2001).
[4] S. Fazinić, M. Jaskšić, L. Mandić, and J. Dobrinić, Phys. Rev. A **74**, 062501 (2006).
[5] V. Horvat, R. L. Watson, and Y. Peng, Phys. Rev. A **74**, 022718 (2006).